RESEARCH PAPER

Electrochemical synthesis of magnetite and maghemite nanoparticles using dissymmetric potential pulses

A. Rodríguez-López · A. Paredes-Arroyo · J. Mojica-Gomez · C. Estrada-Arteaga · J. J. Cruz-Rivera · C. G. Elías Alfaro · R. Antaño-López

Abstract Magnetic iron oxide nanoparticles of controlled size distribution were electrochemically synthesized applying a dissymmetric pattern of potential pulses to iron-based electrodes in aqueous media. The best pattern was determined through a design of experiments based on a previous voltammetric study. The applied method conveys an optimization of previous methods which employed direct or symmetric alternate potentials. XRD results indicate that magnetite phase is favored to anodic potentials larger −0.2 V versus SSE. TEM images show quasi spherical particles with size ranging from 10 to 50 nm, depending on the synthesis conditions, which agrees with size estimated from diffractograms. EDS indicate that the electrolyte is not totally eliminated by washing although its content is lower than 1 %.

A. Rodríguez-López · A. Paredes-Arroyo ·
J. Mojica-Gomez · C. Estrada-Arteaga ·
R. Antaño-López (✉)
Centro de Investigación y Desarrollo Tecnológico en Electroquímica, S. C., Parque Tecnológico Querétaro, Sanfandila, Pedro Escobedo, C.P. 76703 Querétaro, Mexico
e-mail: rantano@cideteq.mx

A. Rodríguez-López
Centro Nacional de Metrología, Km 4.5 Carretera a los Cués Municipio, El Marqués, C.P. 76246 Querétaro, Mexico

J. J. Cruz-Rivera · C. G. Elías Alfaro
Instituto de metalurgia, Facultad de Ingeniería, Universidad Autónoma de San Luis Potosí., Sierra Leona No. 550, Lomas segunda sección, C.P. 78210 San Luis Potosí, SLP, Mexico

Introduction

Magnetite (Fe_3O_4) is a material having nowadays both industrial and scientific interest. In the environmental field, it is widely used for metal separation from wastewater. In the industry, it is extensively used in magnetic ink (Cornell and Schwertmann 2003). In recent years, this material has been proposed for biomedical applications such as cell targeting, cell separation, drug delivery, or hyperthermia (Tsouris et al. 2001a, b; Ying et al. 2002; Marques et al. 2008).

Because of this diversity of applications, interest in magnetite nanoparticles has recently grown. Although this material has been studied for many years, the fact of study of nanoparticles involve new knowledge because it is reported that nanoparticles exhibit electrical, chemical, magnetic, and optical properties different from those presented in bulk size (Pascal et al. 1999; Santos et al. 2008; Teja and Koh 2009).

Even though there are several methods for magnetite synthesis (Tartaj et al. 2003; Franger et al. 2007; Teja and Koh 2009), the chemical co-precipitation

method is actually the most used. This method has been improved in the last years; however, there are already some problems to solve, particularly concerning the control of the particle size and its distribution. This is the reason why alternative methods, including the electrochemical ones, have been investigated.

The electrochemical methods to synthesize magnetite present some advantages over other methods; the most important are the high purity of the product and the control of the particle size achieved by adjusting the current or the potential applied to the system (Tsouris et al. 2001a, b; Franger et al. 2004; Cabrera et al. 2008).

Several works have reported electrochemical synthesis of magnetite: Tsouris et al. (2001a, b) claimed for a method and apparatus to electrolytically produce high-purity magnetite particles. This method consists of submerging a pair of metal electrodes in a temperature-controlled electrolytic solution and applying a direct voltage to the electrodes for a period of time sufficient to produce the metal oxides particles. Tsouris mentioned that the distance between electrodes of 5 cm is a skill in the art and observed that the pH of the sodium chloride solution increased from 6–7 to 10–12 after 940 s, applying voltages from 2.5 to 7.5 V. Ying et al. (2002) reported an electrochemical method for the formation of magnetite particles applying a constant voltage during 940 s to two electrodes of carbon steel. Franger et al. (2004) studied the electrochemical synthesis of magnetite nanoparticles in alkaline aqueous solutions with complexing agents, indicating that the role of the complexing entities is purely kinetic. Franger applied 5 V between working and counter electrode or 50 mA as a constant current and observed oxidation of the iron anode when hydrogen gas evolution occurred at cathode. Cabrera et al. (2008) synthesized magnetite nanoparticles electrochemically using two iron electrodes separated at 1 cm in 0.04 M aqueous solution of Me_4NCl. She ranged the potential between 1 and 15 V and current density between 10 and 200 mA/cm^2. The mean size of the particles was between 20 and 30 nm with quite uniform and spherical size. Cabrera concluded that the distance between electrodes is critical for the synthesis; in her case, it should be smaller than 5 cm. About the reaction mechanism, it is mentioned that magnetite is produced through $Fe(OH)_3$ reduction. Marques et al. (2008) reported the electroprecipitation of magnetite nanoparticles in ethanol using two carbon cylinders as electrodes and $Fe(NO_3)_3$ at different content in ethanol as iron precursor; the voltage between the electrodes was kept constant at 62 V. They found nanoparticles of magnetite with the standard deviation of the size particle around 20 %, concluding that the low dispersion can be explained by the precipitation phenomenon that occurs in a very restricted region during a very short time in agreement with Pascal et al. (1999) for the synthesis of γ-Fe_2O_3 nanoparticles. Ibrahim et al. (2009) continued this study in alcohol medium using graphite rods as anode and cathode and $Fe(NO_3)_3$ solutions at different concentrations. They explored the potential range from 20 to 60 V.

As can be seen, the methodology to synthesize nanoparticles of magnetite by electrochemical route is still under investigation. The methods reported use huge energy quantities involving diffusion process and no fine size control is reached. In order to improve the actual methodology, a new method to produce electrochemically magnetite nanoparticles is proposed by applying dissymmetric potential pulses to iron electrodes in aqueous media. The obtained powders are characterized by XRD, TEM, and EDS.

Experimental

Electrochemical system

A three-electrode cell of 50-mL capacity was employed for the experiments. The working electrode was high-purity iron (Goodfellow, 99.5 %) with 1 cm^2 of geometric area. 2 cm^2 of high-purity iron was used as a counter electrode for the generation of the magnetite nanoparticles. For the selection of potentials and times for the synthesis, a 4-cm^2 99.95 % palladium foil was used as a counter electrode. The reference was a mercury-mercurous sulfate-saturated electrode (SSE). KCl 0.5 M was used as an electrolyte to decrease the solution's resistance and to avoid migration effects of electroactive species. The distance between working and counter electrodes was adjusted to 3 cm.

The solutions were prepared using ACS grade reagents and deionized water. The experiments were performed at environmental temperature and atmospheric pressure.

Electrochemical synthesis

Three to five minutes were spent to achieve the stabilization of the system before each experiment.

The solution was maintained without stirring. Linear voltammetry at 2 mV/s was carried out to identify and to select the reduction and oxidation potentials of iron ions. In the same way, chrono amperometric studies were performed to select the time for the potential pulses. With the information about potentials and times for the pulses, a design of experiments was elaborated by means of the jmp4 program by SAS institute Co, where a 2^n model was employed and n stands for the number of variables, four in this case: anodic potential, cathodic potential, anodic time, and cathodic time. To each variable, an upper and a lower limit was assigned. In addition, one intermediate point was selected. Finally, one replicate for experiment was required. Thus, a design of experiments with 34 tests was obtained. The total time for all the experiments was 1 h.

The synthesis was carried out using a potentiostat/galvanostat PARSTAT 2273 (Princeton Applied Research). In order to measure the potential of counter electrode during the synthesis, a second reference electrode (SSE) was added to the electrochemical system and connected to a Fluke 273 multimeter.

Powder's characterization

The suspension was washed three times with water and a final wash was made with ethanol using a Hermle centrifuge, model Z206A, at 5,000 rpm for 15 min to separate the solid from the liquid part at each wash. After ethanol washing, the product was lyophilized (Labconco, freezone 2.5) during 60 min using the serpentine at −50 °C. The obtained powder was characterized by XRD, TEM, and EDS.

XRD experiments were performed immediately after the powders were obtained to minimize possible oxidation of the powders because no surfactants were added to the system during or after the synthesis. This technique was used to identify the crystalline phases of the iron oxide powders, recording the diffractogram from 20° to 90° 2θ in a Bruker D8 advance appliance, with a Cu K$_\alpha$ radiation. The diffractograms were used to estimate the crystal size from the broadening of the (3 1 1) plane signal by the Scherrer equation:

$$d = \frac{0.89 \cdot \lambda}{\beta \cdot \cos \theta}$$

where d is the mean length of the crystal, λ is the wavelength of radiation, β is the line broadening, and θ is the diffraction angle.

To analyze size and shape of the particles, TEM (JEM 1230 JEOL) experiments were carried out. The samples were prepared by making a suspension from the powder in ethanol, sonicating during 10 min, followed up by the addition of one drop of this suspension onto a carbon-coated copper grid and allowing the solvent evaporation. The mean particle size and the size distribution were estimated by measuring the internal dimension of at least 120 particles.

The same arrangement and samples used for TEM tests were employed for EDS experiments. That technique gave information about the proportion of the elements at nanoparticles surface, contributing to the estimation of the possible phases in the powders.

Results and discussion

Electrochemical synthesis

Selection of potential and time for the pulses

The voltammetry in the cathodic scan to select the potentials of the pulses is shown in Fig. 1. It can be seen that there are two well-defined reduction peaks. The first one is wide and presents a maximum at −1.2 V. It is attributed to the reduction of ferric to ferrous ion (Periasamy et al. 1996); Such a wide peak can be attributed to the existence of different structures containing the ferric ion. The second peak is narrower and presents a maximum at −1.4 V. It is assigned to the reduction of ferrous ion to metallic iron (Periasamy et al. 1996). The presence of both peaks suggests that the electrolyte oxidized the iron to ferric species because of the corrosion voltage during the
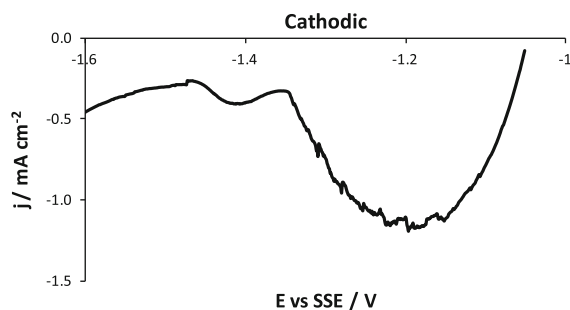
Fig. 1 Linear voltammetry obtained in KCl 0.5 M. Scan in cathodic sense at speed of 2 mV/s

stabilization time (pH 5.8). The maximum of both peaks were chosen as minimum and maximum values to apply the potential pulses.

The scan in the anodic sense is shown in Fig. 2. In this case, there is no appreciable oxidation peak; however, it is possible to note a slope change at approximately −0.3 V, which indicates a change in the oxidation process. Anodic potentials around this value were chosen to propose a design of experiments to apply the pulses: −0.7 and +0.3 V (before and after this slope change). It is worth to mention that during this scan, bubbles at the counter electrode (operating as cathode at that moment) were observed, evidencing the water electrolysis.

Another important parameter in the proposed method of synthesis is the time during which the potential pulses will be applied. During the chrono amperometric tests, as awaited, in the beginning, the current increased abruptly then decreased and increased again (both anodic and cathodic sense). In order to avoid the diffusion of species to the bulk, the time around the point, where the current starts to increase again, was selected. Hence, for anodic pulse, 2 and 5 s were selected, while for cathodic pulse, 1 and 3 s were chosen in the design of experiments.

Application of potential pulses

The experiments applying potential pulses were carried out following the design of experiments shown in Table 1. The pH of the solution was measured at the beginning and at the end of the experiments; in general, it was found that it changes from 5.8 to 9.8. This increase in the pH solution is mainly attributed to water electrolysis that occurs at iron counter electrode when it is functioning as cathode. It is reported (Ying
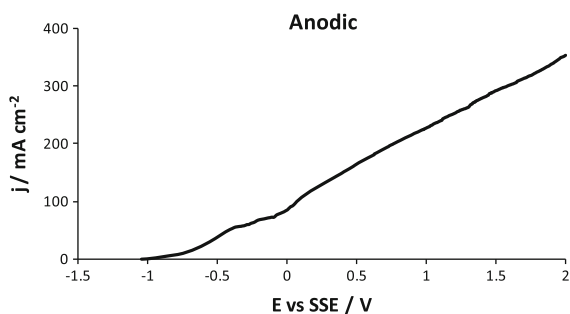
Fig. 2 Linear voltammetry obtained in KCl 0.5 M. Scan in anodic sense at speed of 2 mV/s

et al. 2002; Cabrera et al. 2008) that this reaction increases the pH and furnishes the hydroxyl ions needed to form ferric hydroxide, which is precursor of magnetite. In addition, these papers indicated that the hydroxyl ions generated at cathode must travel to the anode to form the ferric hydroxide.

In our system, the electrodes are changing polarity; thus, the working electrode acts as anode for a time, generating ferrous and ferric ions, afterward as cathode, generating hydroxyl ions to form chemically ferric hydroxide and, at the same time, reducing that hydroxide to magnetite. In this way, hydroxyl ions generated at the cathode are not longer traveling to the other electrode, saving in consequence the energy related to this mass transfer.

According to references (Ying et al. 2002; Cabrera et al. 2008), the reactions occurring at counter electrode are relevant to the magnetite synthesis, particularly the water hydrolysis, which provides the hydroxyl ions necessary to form the ferric hydroxide. It is worth to note that according to potentiostat operation principle, for a three-electrode arrangement, the potential of the counter electrode is adjusted to reach the required potential at the working electrode interface. So, the counter electrode potential is depending on the working electrode potential. Thus, a SSE was added to the system to monitor the counter electrode potential behavior during the synthesis. In Fig. 3, a typical behavior of working and counter electrode potential during the first minute of synthesis is shown.
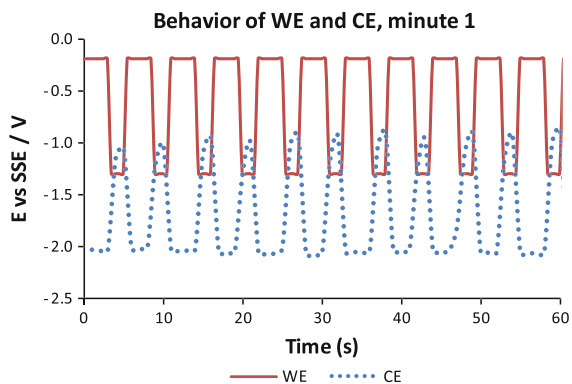
From Fig. 3, it is possible to deduce that working electrode is the one which provides the iron ions to the system because comparing the potentials when the polarity of both electrodes is anodic in the cycles, its potential is bigger than that of the counter electrode. For cathodic polarization, it is feasible to note that counter electrode present the highest values, which indicate that this electrode generate mainly the hydroxyl ions.

Formation of magnetite nanoparticles

For all the experiments, the solution, initially color-less, presents a change of color after some few seconds (red–brown–black), mainly in the region close to the electrodes interface. This color depends on the synthesis conditions for some experiments the solution and the isolated powder had a brown-red color for others the color is purely black, indicating that

Table 1 Description of the experiments design for the synthesis of magnetite applying potential pulses

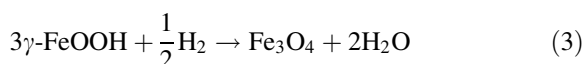| Experiment	Anodic potential (V vs SSE)	Cathodic potential (V vs SSE)	Anodic time (s)	Cathodic time (s)	Experiment	Anodic potential (V vs SSE)	Cathodic potential (V vs SSE)	Anodic time (s)	Cathodic time (s)
1	−0.7	−1.2	2	3	18	0.3	−1.2	2	3
2	0.3	−1.4	2	1	19	−0.7	−1.4	5	1
3	0.3	−1.4	5	3	20	0.3	−1.4	2	3
4	−0.7	−1.2	5	1	21	−0.7	−1.4	5	3
5	−0.7	−1.4	2	3	22	−0.7	−1.4	2	1
6	−0.7	−1.4	5	3	23	0.3	−1.2	5	3
7	0.3	−1.4	5	1	24	0.3	−1.2	2	1
8	0.3	−1.2	5	1	25	0.3	−1.2	5	3
9	0.3	−1.4	5	3	26	−0.7	−1.4	2	3
10	−0.7	−1.2	5	3	27	−0.2	−1.3	3.5	2
11	0.3	−1.2	2	1	28	−0.7	−1.2	2	3
12	0.3	−1.2	2	3	29	−0.7	−1.2	2	1
13	−0.7	−1.2	2	1	30	−0.7	−1.2	5	1
14	0.3	−1.4	2	3	31	0.3	−1.2	5	1
15	−0.7	−1.2	5	3	32	0.3	−1.4	2	1
16	−0.2	−1.3	3.5	2	33	−0.7	−1.4	5	1
17	0.3	−1.4	5	1	34	−0.7	−1.4	2	1

Fig. 3 Typical behavior of working and counter electrode potential during the first minute. Potential pulses condition for working electrode: E_{anodic} −0.2 V versus SSE for 3.5 s, $E_{cathodic}$ −1.3 V versus SSE for 2 s
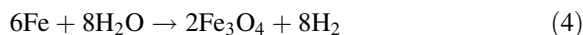
magnetite is formed preferentially (Cornell and Schwertmann 2003).

At present, there are basically two reaction mechanisms that have been proposed in the literature for the magnetite formation during electrochemical synthesis. The first mechanism proposes that magnetite is produced through an iron(III) oxyhydroxide intermediate. Franger et al. (2004) studied the electrochemical synthesis of magnetite nanoparticles in alkaline

aqueous solutions containing complexing agents. It is indicated that there are three reactions involved at magnetite formation: oxidation of iron at anode (step 1), water electrolysis at cathode (step 2), and a chemical reaction at solution (step 3).

$$Fe + 3OH^- \leftrightarrow \gamma - FeOOH + H_2O + 3e^- \quad (1)$$

$$H_2O + e^- \leftrightarrow \frac{1}{2}H_2 + OH^- \quad (2)$$

$$3\gamma\text{-FeOOH} + \frac{1}{2}H_2 \rightarrow Fe_3O_4 + 2H_2O \quad (3)$$

where the global reaction is

$$6Fe + 8H_2O \rightarrow 2Fe_3O_4 + 8H_2 \quad (4)$$

Franger indicated that the distance between electrodes is important at synthesis, and mentioned that the dihydrogen generated at counter electrode should have an important role in magnetite formation, and that its diffusion through the solution allows reducing partially the γ-FeOOH formed at anode to form magnetite. This mechanism presents the problem at the assumption that hydrogen gas generated in the electrode interface must travel to the bulk solution to reduce the oxyhydroxide, while it is well known that bubbles evolve from the solution.

The second reaction mechanism, reported by Ying et al. (2002) as well as Cabrera et al. (2008), includes the reduction of ferric hydroxide at cathode. In these papers, they proposed that ferrous and ferric ions are generated at anode (steps 5 and 6); while at cathode, there is a pH increase due to several reactions (steps 2, 7 and 8).

$$Fe \leftrightarrow Fe^{2+} + 2e^- \tag{5}$$

$$Fe^{2+} \leftrightarrow Fe^{3+} + 1e^- \tag{6}$$

$$2H^+ + 2e^- \leftrightarrow H_2 \tag{7}$$

$$4H^+ + O_2 + 4e^- \leftrightarrow 2H_2O \tag{8}$$

According to Cabrera et al. (2008), the hydroxyl ions produced at cathode arrive to the anode's surface by diffusion, providing the basic medium necessary to form iron hydroxide. When the pH of solution raises up to 9, the precipitation of ferric ions as hydroxide is favored following the reaction 9.

$$Fe^{3+} + OH^- \leftrightarrow Fe(OH)_3(s) \tag{9}$$
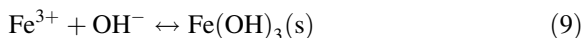
Once the ferric hydroxide has been formed, if solution pH is around 8 or 9, it can be reduced to magnetite (step 10). To achieve this, it is necessary that the hydroxide travel to the cathode to be partially reduced at this electrode (Ying et al. 2002; Cabrera et al. 2008).

$$3Fe(OH)_3(s) + H^+ + e^- \leftrightarrow Fe_3O_4(s) + 5H_2O \tag{10}$$
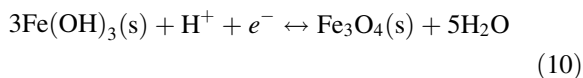
This second mechanism has received some criticism because the $Fe(OH)_3$, which is solid, must travel to the cathode's surface to be reduced to magnetite, which seems unlikely because of the precipitation of that solid.

Based on these assumptions, the proposed reaction mechanism for magnetite formation at our dissymmetrically pulsed system is depicted as follows: when the working electrode has the anode role, ferrous and ferric ions are produced (steps 5, 6), while dihydrogen gas is formed at counter electrode (cathode at this moment) by water electrolysis (step 2). When this pulse ends, the applied potential is changed to make the working electrode works like cathode, while the counter electrode potential moves to anodic values. In this second pulse, hydroxyl ions are formed at working electrode (step 2), which can react with the nearest iron ions produced during the first pulse to form the ferric specie (steps 1 or 9). This ferric species can be then reduced to magnetite in a chemical way (step 3) or during this second pulse (steps 10 and 11).

$$3\gamma\text{-FeOOH} + e^- \leftrightarrow Fe_3O_4(s) + H_2O + OH^- \tag{11}$$
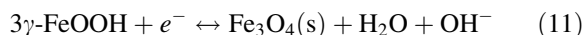
Step 11 was proposed for Amaral and Müller (1999) in different conditions, but we think that this reaction could be occurring in our actual conditions. Also, it is more reasonable to think that this soluble species, and not the solid proposed in the second mechanism, travel to the surface of the cathode and react.

For each experiment, these potential pulses were applied in a cyclic way until 1 h was completed. A typical behavior of these potentials is shown at Fig. 4. It is possible to see in this figure that the working electrode is moving between the potentials required. In contrast, the counter electrode presents changes during the synthesis, particularly when it works as anode: the value of the potential increased from -0.90 to -0.45 V during the first 5 min (time where the change in the solution color is observed from colorless to brown-red). The origin of this change is not clear yet and further studies must be developed to understand this behavior. However, we can advance that it could be attributed to two principal processes: first, at the beginning, the value of the anodic potential is low because small current is needed to reduce particles at working electrode, keeping the potential practically

Fig. 4 Typical behavior of **a** working and **b** counter electrode potential during the experiments. Potential pulses condition for working electrode: E_{anodic} -0.2 V versus SSE for 3.5 s, $E_{cathodic}$ -1.3 V versus SSE for 2 s
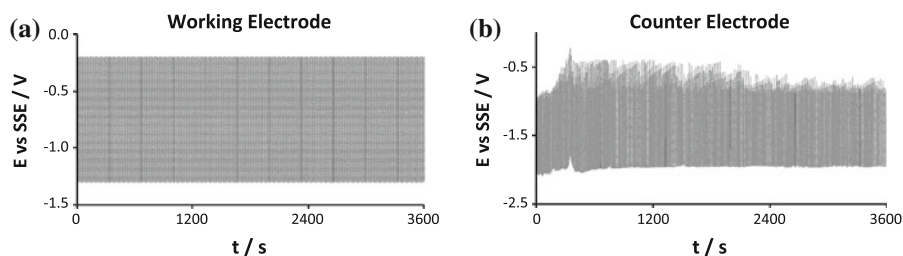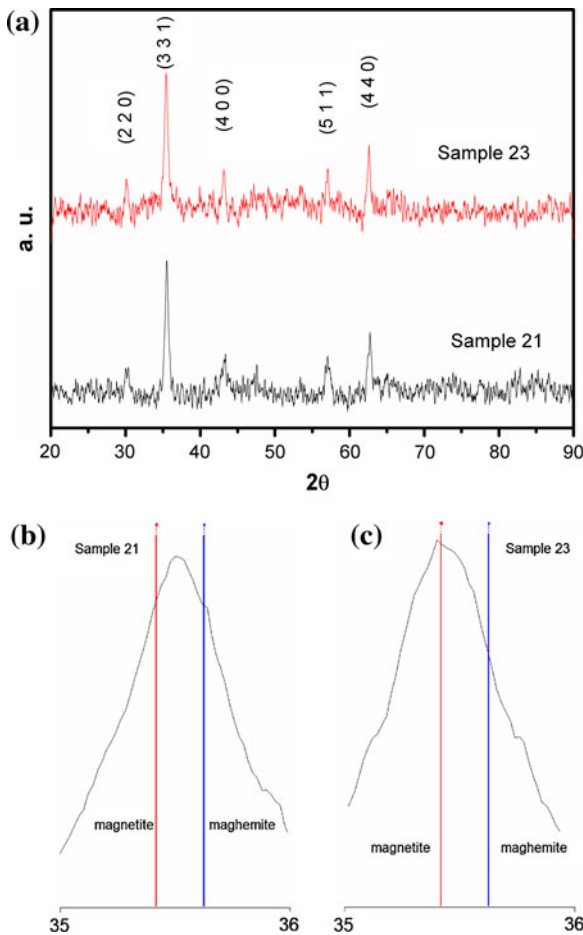
Fig. 5 a X-ray diffraction of nanoparticles formed in experiments. Comparison between diffraction peak against diffraction patterns of magnetite and maghemite. **b** Sample of experiment 21 when −0.7 V versus SSE was the anodic pulse, **c** sample of experiment 23 when 0.3 V versus SSE was used as anodic pulse

constant. At larger times ferric hydroxide is formed and magnetite nanoparticles are produced by its reduction at working electrode, requiring more energy and thus producing a potential drop. Second, the process of water electrolysis that makes the potential changes strongly when the generated dihydrogen bubbles leave the surface.

Characterization of magnetic powders

X-ray diffraction (XRD)

Diffractograms of obtained powders were collected and compared against several iron oxide diffraction patterns (magnetite, maghemite, hematite, and goethite) and

metallic iron. No metallic iron was detected at any sample, indicating that this undesired reaction was absent. This is in agreement with results of Cabrera et al. (2008) where metallic iron was found when the potential between electrodes was extreme (higher than 6 V). The XRD pattern of two iron oxide nanoparticles is shown in Fig. 5a. It is worth to note that analyzed powders presented their peaks between the specific peaks of magnetite and maghemite (Fig. 5b), corresponding to the presence of both phases in the product, a commonly reported situation (Cabrera et al. 2008). In spite of this, some powders presented peaks that clearly can be assigned to the characteristic peaks of Fe_3O_4 (Fig. 5c).

The XRD patterns that were more likely to magnetite were obtained when the anodic potential was the highest with the longest time as well. It could be attributed to a higher pH conditions at interphase during the reduction of ferric hydroxide, favoring to the formation of magnetite over the ferric oxide, the formation of which is favored at less basic pH (Ying et al. 2002; Cabrera et al. 2008). By the Scherrer equation, the crystal size was estimated from the broadening of the (3 1 1) plane, obtaining the values reported in Table 2.

Transmission electron microscopy (TEM)

TEM analysis showed that the powders collected are quasi spherical nanoparticles with sizes similar to those estimated from XRD (Table 2). Images from a sample synthesized to +0.3 V versus SSE as anodic potential during 5 s and −1.2 V versus SSE for 3 s at two different scales are shown in Fig. 6. Here, it is possible to distinguish aggregates of the particles, the shape of size distribution depending on the synthesis conditions.

Comparing the size estimated by TEM against the obtained by XRD, it is possible to observe that although some differences exist; the XRD sizes overlap TEM results, if the twofold standard deviation of TEM measurements is considered, which covers the results with a confidence level of 95 %.

Energy dispersion spectroscopy (EDS)

The elementary composition of nanoparticles was determined by EDS. The results agree with XRD analysis, where for some conditions magnetite phase is favored in the product, while for others a mixture of

Table 2 Estimated size from XRD and TEM of the synthesized nanoparticles at different conditions

Anodic potential	Anodic time (s)	Cathodic potential	Cathodic time (s)	Size (nm)		
				XRD	TEM	TEM$_{std\ dev}$
0.3	5	−1.4	3	14	27	9
0.3	5	−1.2	3	20	29	9
−0.2	3.5	−1.3	2	22	32	9
−0.7	5	−1.2	1	17	29	9

Fig. 6 TEM micrographs of magnetite nanoparticles synthesized at 0.3 V versus SSE for 5 s as anodic pulse and −1.2 V versus SSE for 3 s as cathodic pulse
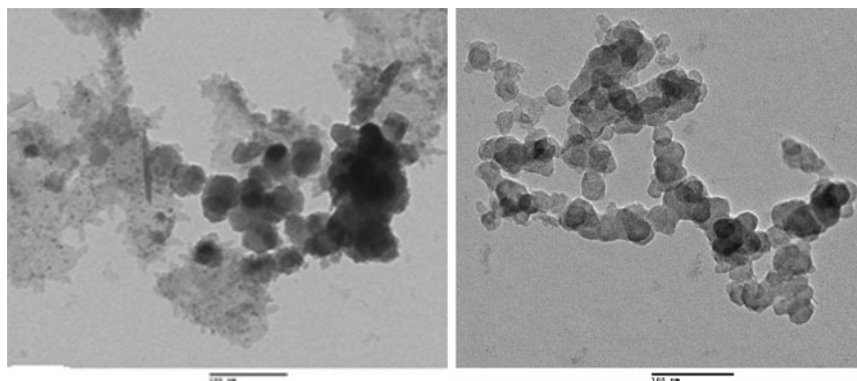
iron oxides is obtained. EDS of a sample is shown in Fig. 7 as an example. It can be seen that also potassium and chloride ions are present as traces due to the electrolyte employed during the synthesis.

Conclusions

Magnetic iron oxide nanoparticles have been successfully synthesized applying dissymmetric potential pulses to iron-based electrodes in aqueous potassium chloride. This permitted to save energy and thus optimize the synthesis. It was found that magnetite nanoparticles formation is favored, while avoiding formation of metallic iron particles with more anodic potentials and longest time, according to the potential and time range explored in our design of experiments. The obtained nanoparticles had a quasi spherical shape and the size—the shape distribution of which depends on the synthesis conditions—ranged from 10 to 50 nm.

Although the determination of the reaction mechanism needs more studies to achieve a full understanding of the process, a mechanism is proposed based on our results and on references. This mechanism indicates that mass transfer is minimized.
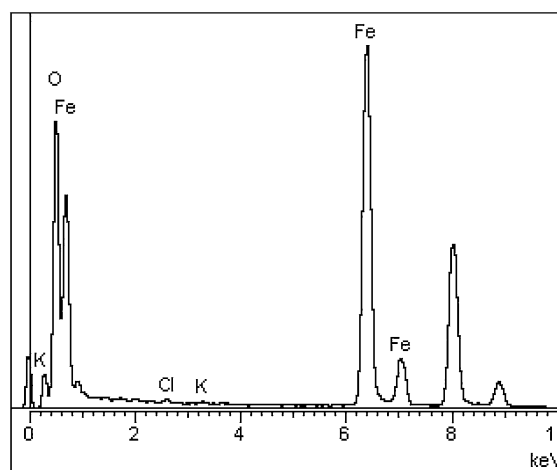
Fig. 7 EDS results for a sample synthesized using 0.3 V versus SSE for 5 s as anodic pulse and −1.2 V versus SSE for 3 s as cathodic pulse

References

Amaral ST, Müller IL (1999) Electrochemical behaviour of iron in NaOH 0.01 mol/L solutions containing variable amounts of silicate. J Braz Chem Soc 10(3):8

Cabrera L, Gutierrez S et al (2008) Magnetite nanoparticles: electrochemical synthesis and characterization. Electrochim Acta 53:6

Cornell RM, Schwertmann U (2003) The iron oxides. Structure, properties, reactions, occurrences and uses. Wiley-VCH, Weinheim

Franger S, Berthet P et al (2004) Electrochemical synthesis of Fe_3O_4 nanoparticles in alkaline aqueous solutions containing complexing agents. J. Solid State Electrochem 8:6

Franger S, Berthet P et al (2007) Large influence of the synthesis conditions on the physico-chemical properties of nano-structured Fe_3O_4. J Nanopart Res 9:14

Ibrahim M, Serrano KG et al (2009) Electro-precipitation of magnetite nanoparticles: an electrochemical study. Electrochim Acta 55:4

Marques RFC, Garcia C et al (2008) Electro-precipitation of Fe_3O_4 nanoparticles in ethanol. J Magn Magn Mater 320:5

Pascal C, Pascal JL et al (1999) Electrochemical synthesis for the control of γ-Fe_2O_3 nanoparticle size. Morphology, microstructure, and magnetic behavior. Chem Mater 11(1):7

Periasamy P, Babu BR et al (1996) Cyclic voltammetric studies of porous iron electrodes in alkaline solutions used for alkaline batteries. J Power Sources 58:6

Santos FJ, Varanda LC et al (2008) Synthesis and electrochemical behavior of single-crystal magnetite nanoparticles. J Phys Chem 112:6

Tartaj P, Morales MdP et al (2003) The preparation of magnetic nanoparticles for applications in biomedicine. J Phys D: Appl Phys 36:16

Teja AS, Koh P-Y (2009) Synthesis, properties, and applications of magnetic iron oxide nanoparticles. Prog Cryst Growth Charact Mater 55:24

Tsouris C, DePaoli DW et al (2001) Method and apparatus to electrolyticalle produce high-purity magnetite particles. US, UT Battelle, LLC, p 9

Tsouris C, DePaoli DW et al (2001) Electrocoagulation for magnetic seeding of colloidal particles. Colloids Surf A: Physicochem Eng Aspects 177:11

Ying T-Y, Yiacoumi S et al (2002) An electrochemical method for the formation of magnetite nanoparticles. J Dispers Sci Technol 23(4):8